

Preparation of 3-7 MeV Neutron Source and Preliminary Results of Activation Cross Section Measurement

T. Furuta, H. Sakane*, T. Masuda, Y. Tsurita, A. Hashimoto, N. Miyajima,
M. Shibata*, H. Yamamoto* and K. Kawade*

Department of Nuclear Engineering, Nagoya University

**Department of Energy Engineering and Science, Nagoya University*

e-mail:h982422m@sunspot.eds.ecip.nagoya-u.ac.jp

A d-D gas target producing monoenergetic neutrons has been constructed for measurement of activation cross sections in the energy region of 3 to 7 MeV at Van de Graaff accelerator of Nagoya university. Neutron spectra and neutron fluxes were measured as a function of the incident deuteron energy. Preliminary results of activation cross sections were obtained for reactions $^{27}\text{Al}(n,p)^{27}\text{Mg}$, $^{27}\text{Al}(n,\alpha)^{24}\text{Na}$, $^{47}\text{Ti}(n,p)^{47}\text{Sc}$, $^{56}\text{Fe}(n,p)^{56}\text{Mn}$, $^{58}\text{Ni}(n,p)^{58}\text{Co}$ and $^{64}\text{Zn}(n,p)^{64}\text{Cu}$. The results are compared with the evaluated values of JENDL-3.2. A well-type HPGe detector was used for highly efficient detection.

1 Introduction

A knowledge of activation cross section data for neutron energies up to 15 MeV are indispensable for fusion technology, especially for calculations on activation of materials, radiation damage, nuclear heating and so on. Considerable amounts of data exist around 14 MeV. However, in an energy range between 3 and 13MeV, the experimental data are rather scarce owing to the lack of available monoenergetic neutron sources. In the energy range of 5 to 10 MeV, Qaim *et al.*⁽¹⁾ also reported on the characteristics of a deuteron gas target and cross sections of nickel isotopes using it. In this work, we measured the (n,p) and (n, α) reaction cross sections. A d-D gas target was constructed for production of the monoenergetic neutrons of 3 to 7 MeV energy region, and investigated the characteristics of the neutron sources: neutron spectra and flux.

2 Experimental

2.1 Gas target

An exploded view of a gas target assembly is shown in Fig.1. The target consists of a small Al cell (30-mm-innerlong. 8-mm-innerdiam. 1-mm-thick) which is filled with

D_2 gas at 1.6 kg/cm^2 . The cell is separated the vacuum and the gas area with a $2.2\text{-}\mu\text{m}$ -thick Havar foil. The deuteron beam from the Van de graaff accelerator produces neutrons in the cell via the $D(d,n)^3\text{He}$ reaction. Incident d^+ beam energy and intensity were $1.5 \sim 3.5 \text{ MeV}$ and about $1.5 \mu\text{A}$, respectively. The cell is cooled by a jet of air. The degradation of the deuteron energy in the Havar foil and the D_2 gas was calculated using the range-energy data⁽²⁾ as shown in Fig.2.

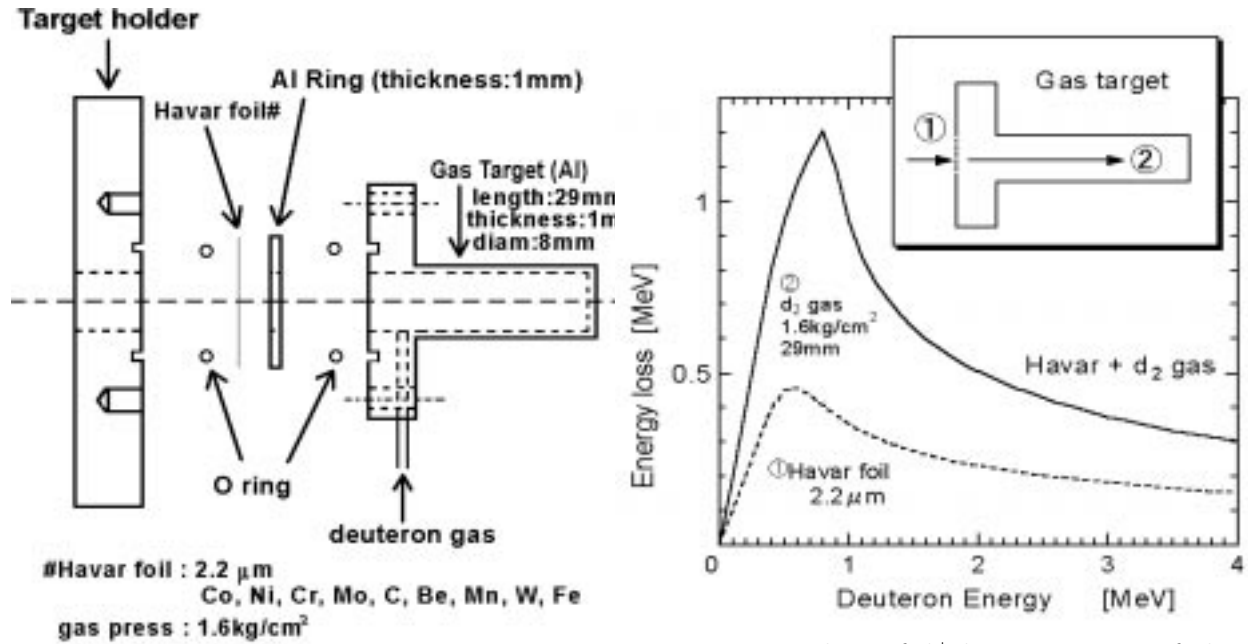


Fig. 2: Energy loss of d^+ beam in Havar foil and D_2 gas

Fig. 1: Exploded view of gas target assembly

2.2 Neutron Spectra and Flux

Neutron spectra at 1m and zero degree with respect to the d^+ beam and at deuteron energy of 1.5 up to 3.5MeV were measured using the organic liquid scintillator NE213 encapsulated by an aluminum cell (50-mm-high , 50-mm-diam.), by mean of the pulse shape discrimination technique.

The neutron flux was measured with use of the standard reaction $^{115}\text{In}(n,n')^{115m}\text{In}$ ($T_{1/2} = 4.486\text{h}$), whose cross section is the evaluated in JENDL-3.2. For a deuteron energy of 2.5 MeV , a typical value of $2.3 \times 10^6 \text{ [n/cm}^2 \text{ s}/\mu\text{A}]$ was obtained at 1.2 cm from the surface of the cell.

The obtained neutron spectra are shown in Fig.3. Quasi-monoenergetic neutrons are clearly seen. However some contributions of low-energy neutrons are also seen. As the produced neutron energy increased, the component of low-energy neutrons increased.

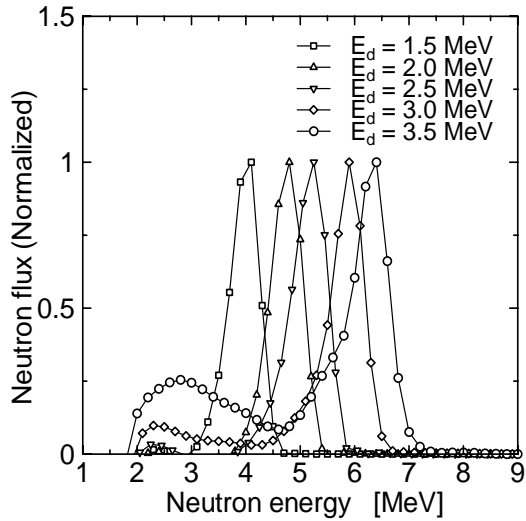


Fig. 3: Measured Neutron spectra

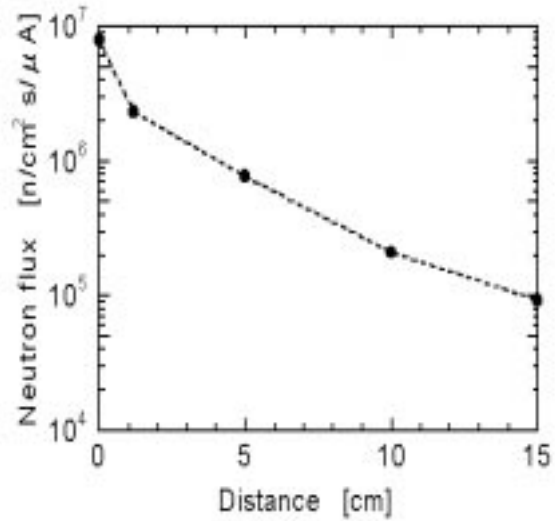


Fig. 4: Measured neutron flux as a function of the distance between the surface of the gas target and a sample.

The ratio of scattered neutrons to total is about 35%. It is necessary for the reliable measurement of cross sections to correct the contribution of low-energy neutrons.

As shown in Fig.4, neutron flux is dependent on the distance between the surface of the cell and sample. Since the neutron flux was obtained about 10^7 unit, sub-mb cross sections can be measured.

3 Cross Section Measurement

We measured activation cross sections of six reactions, $^{27}\text{Al}(n,p)^{27}\text{Mg}$, $^{27}\text{Al}(n,\alpha)^{24}\text{Na}$, $^{47}\text{Ti}(n,p)^{47}\text{Sc}$, $^{56}\text{Fe}(n,p)^{56}\text{Mn}$, $^{58}\text{Ni}(n,p)^{58}\text{Co}$ and $^{64}\text{Zn}(n,p)^{64}\text{Cu}$ by the activation method. Samples were irradiated at 0 degree to d^+ beam and 1.2cm from the end of the D_2 cell by using a pneumatic sample transport system. The samples of $10\text{mm} \times 10\text{mm}$ and 1mm^t were sandwiched between two In foils of $10\text{mm} \times 10\text{mm}$ and 0.5mm in thickness. To monitor the fluctuation of neutron flux, a multi-channel scaling measurement was carried out at an interval of every 10s with a plastic scintillation detector. The induced activities were measured with a well-type and 22% HPGe detectors. The efficiency of both detectors is determined by the calibration method⁽³⁾. Decay parameters of the radioactivity are listed on Table 1.

The following principle corrections were made: (1) contribution of low energy neu-

trons, (2) time fluctuation of neutron flux, (3) deviation of γ -ray detection efficiency due to sample thickness, (4) self-absorption of γ -rays, (5) counting loss due to coincidence sum effect. Details of the corrections are described elsewhere⁽³⁾.

The total errors (δ_t) were described by combining the experimental errors (δ_e) and the errors of nuclear data (δ_r) in quadratic : $\delta_t^2 = \delta_e^2 + \delta_r^2$.

The results for six reactions are shown in Fig.6. They are compared with the evaluated value of JENDL-3.2 and previous works⁽⁴⁾. The experimental cross sections of $^{27}\text{Al}(n,p)^{27}\text{Mg}$, $^{47}\text{Ti}(n,p)^{47}\text{Sc}$, $^{58}\text{Ni}(n,p)^{58}\text{Co}$, and $^{64}\text{Zn}(n,p)^{64}\text{Cu}$ are well agreement with the evaluated value of JENDL-3.2. On the other hand the results of $^{27}\text{Al}(n,\alpha)^{24}\text{Na}$ and $^{56}\text{Fe}(n,p)^{56}\text{Mn}$ in the low energy region (points indicated by arrows), are 10 ~ 100 times larger than the JENDL-3.2.

Table 1. Measured reactions and decay parameters

Reaction	Half life	E_γ	I_γ	Q-value
$^{27}\text{Al}(n,p)^{27}\text{Mg}$	9.458 m	843.7 keV	73 %	-1827.9 keV
$^{27}\text{Al}(n,\alpha)^{24}\text{Na}$	14.959 h	1368.6 keV	99.994 %	-3132.9 keV
$^{47}\text{Ti}(n,p)^{47}\text{Sc}$	3.3492 d	159.3 keV	68.3 %	182.2 keV
$^{56}\text{Fe}(n,p)^{56}\text{Mn}$	2.5785 h	846.7 keV	98.87 %	-2913.0 keV
$^{58}\text{Ni}(n,p)^{58}\text{Co}$	70.82 d	810.7 keV	99.45 %	400.7 keV
$^{64}\text{Zn}(n,p)^{64}\text{Cu}$	12.700 h	511 keV	17.4 % [†]	203.4 keV

[†] annihilation of β^+ -ray

4 Discussion

The results of $^{27}\text{Al}(n,\alpha)^{24}\text{Na}$ and $^{56}\text{Fe}(n,p)^{56}\text{Mn}$ in the low energy region are 10 ~ 100 times larger than the JENDL-3.2. The probable reason for the deviation of the above mentioned two reactions is to be due to the contribution of higher side neutron tail of each peak in Fig.3 which is caused by the energy straggling of a d^+ particle through the Havar foil and D_2 gas.

5 Conclusion

The deuteron gas target was constructed for production of the monoenergetic neutrons. The neutron flux was obtained to be $2.3 \times 10^6 [\text{n}/\text{cm}^2 \text{ s}/\mu\text{A}]$ at 1.2cm in 0 degree with respect to the incident 2.5 MeV deuteron beam. Activation cross sections can be measured down to 1 mb using a well-type HPGe detector. By correcting above mentioned five factor in chapter 3 properly, experimental cross section data of $^{27}\text{Al}(n,p)^{27}\text{Mg}$,

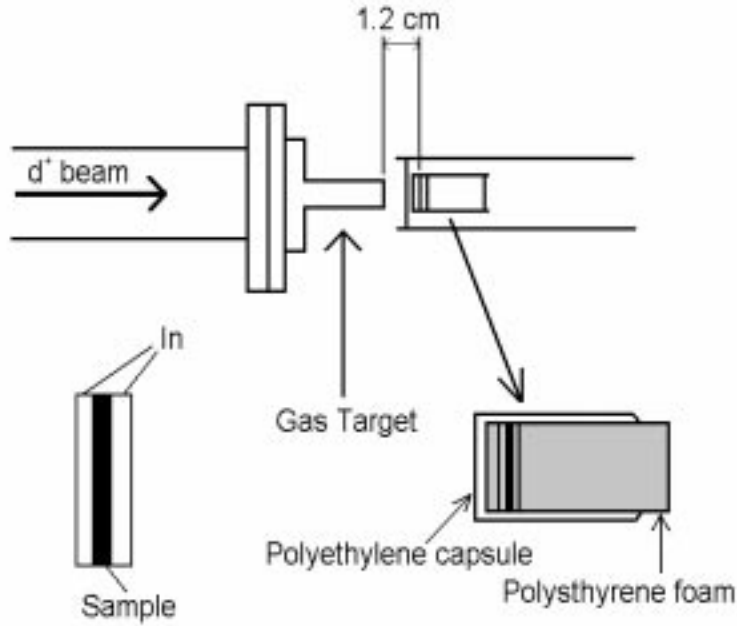


Fig. 5: Pneumatic sample transport system

$^{47}\text{Ti}(n,p)^{47}\text{Sc}$, $^{58}\text{Ni}(n,p)^{58}\text{Co}$, and $^{64}\text{Zn}(n,p)^{64}\text{Cu}$ are well agreement with the JENDL-3.2. However the energy straggling of the incident deuteron are needed to correct for $^{27}\text{Al}(n,\alpha)^{24}\text{Na}$ and $^{56}\text{Fe}(n,p)^{56}\text{Mn}$ because these excitation functions have a sharp slope. We are now planning to prepare the self-loading target with Ti coated for the neutron production of the energy range 3 to 5MeV.

The following reactions are planned to measure: $^{29}\text{Si}(n,p)^{29}\text{Al}$, $^{31}\text{P}(n,\alpha)^{28}\text{Al}$, $^{41}\text{K}(n,p)^{41}\text{Ar}$, $^{45}\text{Sc}(n,\alpha)^{42}\text{K}$, $^{59}\text{Co}(n,p)^{59}\text{Fe}$, $^{59}\text{Co}(n,\alpha)^{56}\text{Mn}$, $^{75}\text{As}(n,\alpha)^{72}\text{Ga}$, $^{93}\text{Nb}(n,\alpha)^{90m}\text{Y}$ and $^{113}\text{In}(n,n')^{113m}\text{In}$.

References

- [1] Qaim, S.M., et al.: *Nucl. Sci. Eng.*, **88**, 143, (1984)
- [2] Andersen, H.H., Ziegler, J.F.: "*Hydrogen Stopping Powers and Ranges in All Elements*", Pergamon Press, New York(1977)
- [3] Kasugai, Y., et al.: *Ann. Nucl. Energy*, **25**, 23, (1998)
- [4] Mclane, V., et al.: "*Neutron Cross Sections*", Vol.2, Academic Press, New York, (1988)

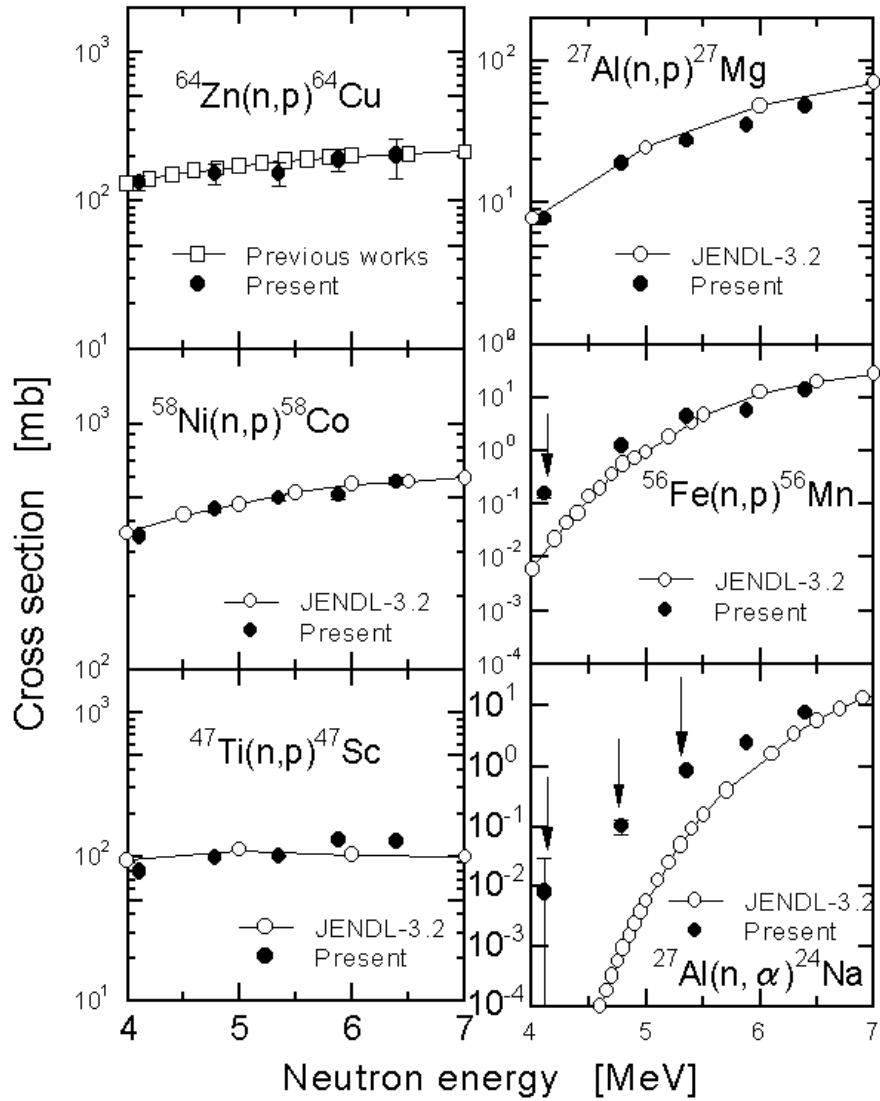


Fig. 6: Experimental cross section data of (n,p), (n, α) reaction.